*Electrochemical and Solid-State Letters,* **12** (3) H60-H63 (2009)
1099-0062/2008/12(3)/H60/4/$23.00 © The Electrochemical Society

# Formation Mechanisms of Low-Resistivity Ni/Pt Ohmic Contacts to Li-Doped p-Type ZnO

**Y. F. Lu, Z. Z. Ye,[z] Y. J. Zeng, L. P. Zhu, J. Y. Huang, and B. H. Zhao**

*State Key Laboratory of Silicon Materials, Department of Materials Science and Engineering, Zhejiang University, Hangzhou 310027, China*

Low-resistivity Ni/Pt ohmic contacts were fabricated on Li-doped, p-type ZnO films using electron-beam evaporation, which were confirmed by the transmission line model technique. The current transport and formation mechanisms of the ohmic contacts were investigated by X-ray photoelectron spectroscopy and temperature-dependent contact resistivity measurements. Activation of acceptors in the ZnO films, formation of Pt–Ni solid solution near the metal surface, and forming a Zn-deficient region near the ZnO surface were considered to result in the improvement of the ohmic contacts. The relatively low barrier height confirmed that the surface states played an important role in the formation of ohmic contacts.
 [DOI: 10.1149/1.3055337] 

Manuscript submitted October 20, 2008; revised manuscript received December 1, 2008. Published December 18, 2008.

ZnO has drawn a lot of attention in recent years due to its potential applications in short-wavelength optoelectronic devices. With a wide bandgap (3.37 eV) and a large exciton banding energy (60 meV), as well as availability of large-area, high-quality single-crystal substrates, ZnO is considered to be more preponderant for high-temperature UV emitters than other compound semiconductors.[1,2] Until now, much progress has been made on fabrication of p-type ZnO, which was long commonly considered to be the major bottleneck of the development of ZnO-based devices.[2-8] However, another important issue to be settled is the fabrication of high-quality ohmic contacts on ZnO materials. There have been some reports on ohmic contacts to n-type ZnO using Ti/Au, Ti/Al, Al/Pt, or Al, etc. as the electrode metals.[9-12] Reports on ohmic contact to p-type ZnO, however, are relatively limited. In our previous study, low-resistivity Li-doped p-type ZnO thin films were obtained by dc reactive magnetron sputtering, and postannealing was carried out to further investigate the p-type conduction mechanism.[2,13,14] In this article we report on low-resistivity Ni/Pt ohmic contacts to Li-doped p-type ZnO thin films. Ni and Pt are chosen as contact metals because of their large work function.

## Experimental

Li-doped ZnO thin films were grown on glass substrates by dc reactive magnetron sputtering. The substrate temperature was 540°C, and the Li content in the sputtering target was 0.1 atom %. Detailed growth procedures were published elsewhere.[2,13] Room-temperature Hall effect measurements showed a hole concentration around $1 \times 10^{17}$ cm$^{-3}$, a Hall mobility of about 2 cm$^2$/Vs, and a resistivity about 40–50 Ω cm. The films also exhibited good crystalline and optical properties.[13,14] Ni (18 nm) and Pt (72 nm) contact metal layers were deposited sequentially by electron-beam evaporation and patterned by photoresist lift-off to form circular transmission line model (CTLM) patterns. The inner radius of the CTLM pad was 50 μm, and the gaps between the inner and the outer pads were 10–60 μm. The pattern image and contact structure can be found elsewhere.[15] Finally, the Ni/Pt contacts were treated by rapid thermal annealing at 500, 550, and 600°C in an $N_2$ environment for 60 s.

The current–voltage (*I-V*) characteristics of these contacts were measured using an Agilent 4155C semiconductor parameter analyzer. The interfacial reactions at the metal–semiconductor interface were characterized by X-ray photoelectron spectroscopy (XPS) (Thermo ESCALAB, USA) using monochromatic Al Kα ($h\nu$ = 1486.6 eV).

[z] E-mail: yezz@zju.edu.cn

## Results and Discussion

Figure 1 shows the *I-V* characteristics of the fabricated contacts. The as-deposited contacts were found to be ohmic. After annealing, the current conducted through the contacts did not show any increase at 500°C. When the annealing temperature increased to 550°C, the current increased. However, the *I-V* plot turned to nonlinear when the annealing temperature reached 600°C. It seems that the current conduction mechanism between the contact metals and ZnO:Li films was changed by annealing at different temperatures.

The specific contact resistivity ($p_c$) was determined from a slope of the measured resistance vs gaps between the CTLM pads.[15] The lowest specific contact resistivity was calculated to be $1.03 \times 10^{-4}$ Ω cm$^2$ after 550°C annealing. Note that the sheet resistance of the Li-doped ZnO films decreased by 3 or 4 magnitudes after annealing at 550°C. It seems that the distinct decrease of specific contact resistivity is related to the reduction of sheet resistance of ZnO films. According to our previous study, postannealing would influence the electrical properties of the ZnO:Li films, and the optimal annealing temperature is around the growth temperature.

Annealing at a proper temperature could dissociate $Li_{Zn}$–$Li_i$ pairs and drive off $Li_i$, resulting in an enhancement of hole concentration and improved p-type conduction.[16] Annealing at a higher temperature would induce a conversion from p-type conduction to n-type, as we observed before, probably due to the re-evaporation of the Li acceptor and aggravated creation of compensating donors.[14] This is consistent with the *I-V* results we observed here. Because the conduction type of ZnO films changes to n-type, it is understandable that the *I-V* plot changes to nonlinear. As the Fermi level of an n-type semiconductor is located near the conduction band minimum,

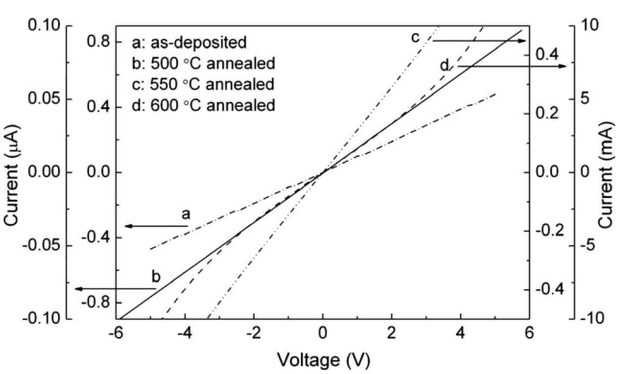


**Figure 1.** *I-V* characteristics of (a) as-deposited and (b) 500°C-, (c) 550°C-, and (d) 600°C-annealed Ni/Pt contacts on Li-doped p-type ZnO. The annealing was carried out in nitrogen environment for 60 s.

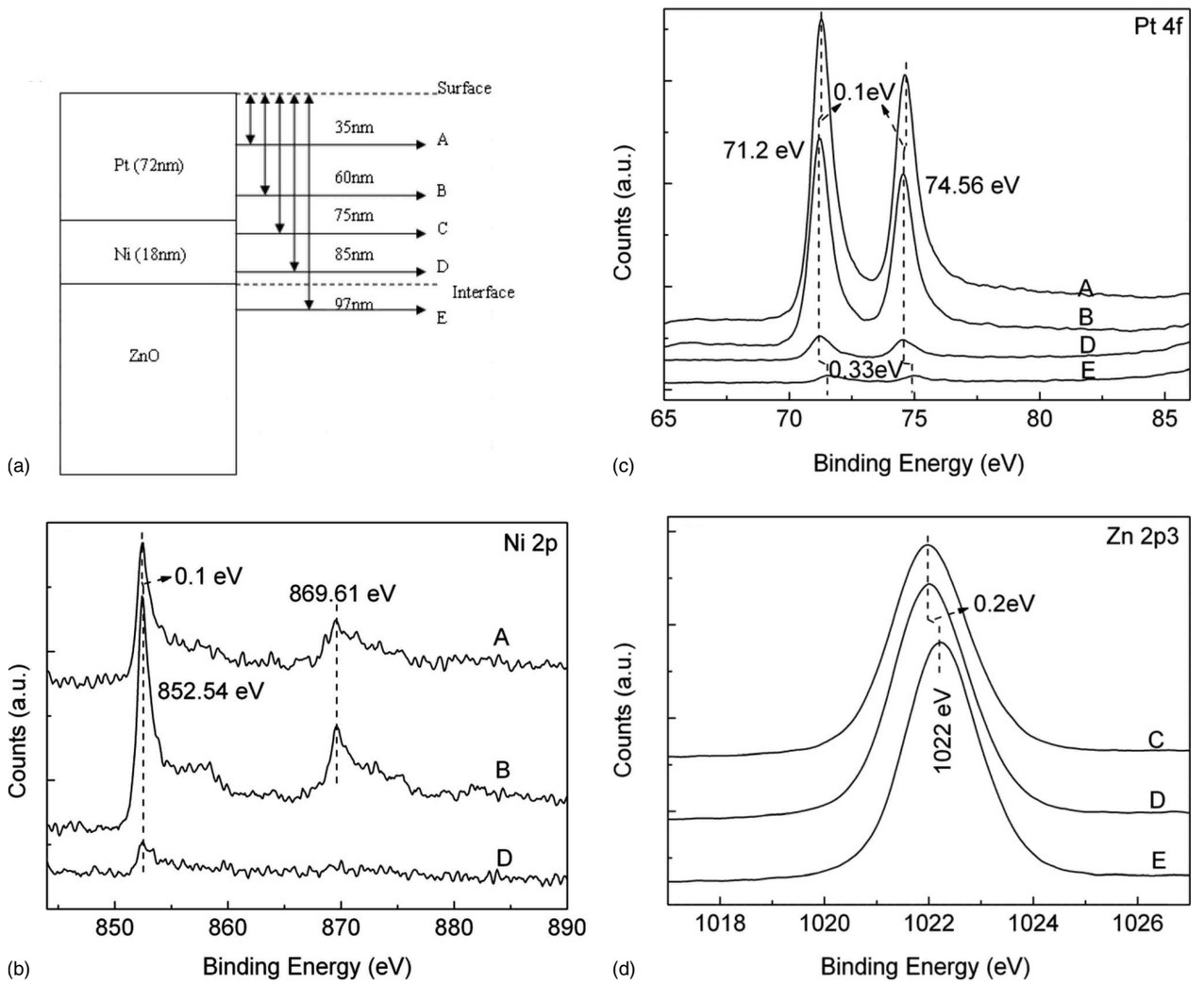


**Figure 2.** XPS depth profile results obtained from the 550°C-annealed Ni/Pt contacts on Li-doped p-type ZnO: schematic depth position (a), and core-level peaks of Ni 2p (b), Pt 4f (c), and Zn 2p3 (d).

the barrier height between the semiconductor and metals with large work function, such as Ni and Pt, increases. Then nonohmic contacts are formed.

The XPS depth profile was recorded to investigate the interfacial reactions between the contact metal and the semiconductor film. As shown in Fig. 2, regions A, B, C, D, and E refer to locations of 35, 60, 75, 85, and 97 nm below the surface, respectively. For 550°C annealed contacts, the XPS spectra revealed out-diffusion of Zn and Ni, and in-diffusion of Pt. These diffusions at the interfaces were accompanied by the formation of Pt–Ni and Pt–Zn solid solutions. Furthermore, a Zn-deficiency region was observed near the metal–ZnO interface at the same time. It is noted that in region B, Ni was found to congregate. This indicates an out-diffusion of Ni atoms, and the appearance of the peak at 869.61 eV suggests that some of the Ni atoms react with oxygen or carbon. The peak near 852.54 eV from region A shifts to the lower binding energy side. In the same region, the binding energy peaks of Pt 4f shift to the higher energy side, indicating formation of Pt–Ni solid solution. This Pt–Ni solid solution could prevent Li atoms in the ZnO layer from re-evaporation during annealing and help to maintain a high acceptor concentration in the ZnO film. Observation of Pt core-level peaks in region E shows in-diffusion of Pt, though the quantity is small, and the peaks of Pt 4f shift to the higher energy side. The core-level peaks of Zn 2p3 in region C or D are 0.2 eV lower than that in region E. These core-level peak behaviors show that Pt may react with Zn, too. Furthermore, it is an evidence for Zn out-diffusion to detect Zn in regions C and D. Therefore, it is reasonable to presume that Zn-deficient region exists near the ZnO surface in which the hole concentration is increased. This is consistent with the above *I-V* measurements and the results reported by others.[17-19] Due to an increase of hole concentration in both the near-surface region and bulk, the barrier height between the metal and semiconductor is reduced, and an obvious decrease of specific contact resistivity is observed in 550°C-annealed samples.

In order to determine the dominant current transport mechanism in the contacts, the specific contact resistivity was measured as a function of temperature. As seen from Fig. 3, the specific contact resistivity of the Ni/Pt contacts annealed at 550°C showed not much change with the increased temperature, indicating a tunneling dominant current transport mechanism. Because the ZnO film was moderately doped, thermionic emission was expected. However, our experimental results showed the tunneling dominance. It is proposed that a Zn-deficient $p^+$-ZnO region existed near the ZnO surface, resulting in the increase of the effective carrier concentration near the ZnO surface. Thus, a Pt–Ni–Zn/$p^+$-ZnO/p-ZnO model can be used to describe the carrier distribution in the ZnO:Li film with

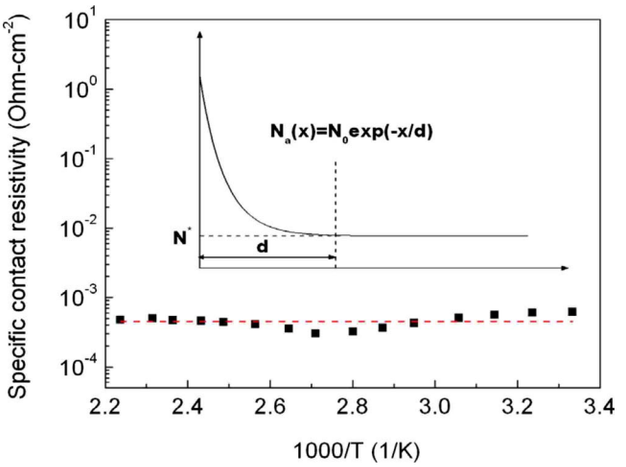


**Figure 3.** (Color online) Plot of the specific contact resistivity as a function of measurement temperatures. The scattered black squares (■) show experimental data, and the dashed line is a theoretical fitting result. The inset shows a schematic carrier concentration depth profile.

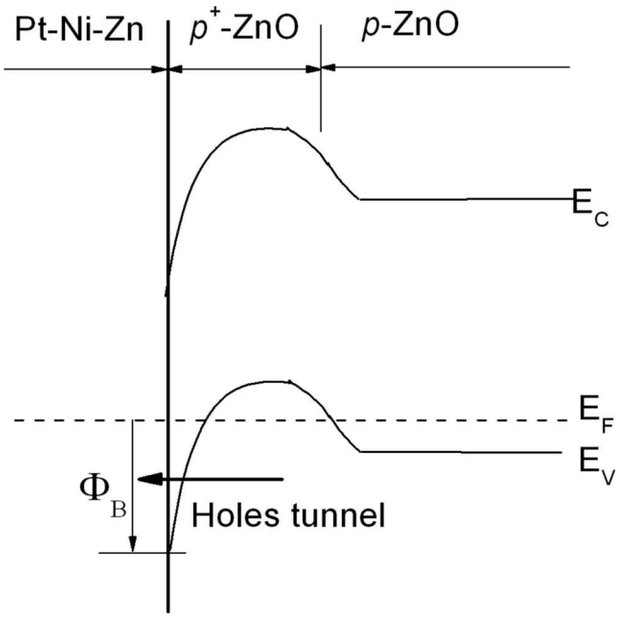


**Figure 4.** Energy diagram of the Pt–Ni–Zn/p$^+$-ZnO/p-ZnO system and schematic ohmic formation mechanism.

Ni/Pt ohmic contacts. The carrier distribution in the p$^+$-ZnO is assumed to be $N_a(x) = N_0 \exp(-x/d)$. The carrier distribution in the ZnO film is given by[20,21]

$$N_{\text{total}} = \frac{\int_0^d N_a(x)dx + \int_d^T N^* dx}{\text{Total thickness}(T)} (\text{cm}^{-3}) \quad [1]$$

where $N_a(x) = N_0 \exp(-x/d)$, $d$ is the effective thickness of the p$^+$-ZnO (which is found to be about 6 nm from XPS), and $N^*$ is the carrier concentration of p-ZnO (from $d$ to $T$). The tunneling parameter ($E_{00}$), which describes the carrier transport at the metal–semiconductor interface, can be defined as[21]

$$E_{00} = \frac{qh}{4\pi}\sqrt{\frac{N_{\text{total}}}{m^*\varepsilon_s}} \quad [2]$$

where $q$ is the electron charge, $h$ is the Planck constant, $m^*$ is the effective hole mass of the semiconductor ($0.59m_e$ for ZnO), and $\varepsilon_s$ is the dielectric constant of the semiconductor ($8.656\varepsilon_0$ for ZnO).[22,23] Based on the field emission mode, the specific contact resistivity is given by[21]

$$\rho_c = \frac{k}{qA^{**}} \exp\left(\frac{q\phi_B}{E_{00}}\right)\left[\frac{\pi T}{\sin(\pi kTC)} - \frac{\exp(-qV_pC)}{kC}\right]^{-1} \quad [3]$$

$$C = \ln(4\phi_B/V_p)/(2E_{00}) \quad [4]$$

where $k$ is the Boltzmann constant, $A^{**}$ is the Richardson constant (32 A cm$^{-2}$ K$^{-2}$ for ZnO), $\Phi_B$ is the barrier height, $T$ is the temperature, and $V_p$ is the energy difference ($E_F$-$E_V$). By fitting the experimental data using Eq. 1-4, (as shown in Fig. 3) the mean carrier concentration in the p$^+$-ZnO region is found to be around $1.57 \times 10^{20}$ cm$^{-3}$, and the effective barrier height is $0.40 \pm 0.03$ eV. This result differs much from the theoretical barrier height calculated from the relation, $\Phi_B = (E_g + \chi)_s - \phi_M$. According to the analysis above, the difference should be ascribed to the surface states induced by interfacial metal diffusions. The energy diagram of this system is schematically shown in Fig. 4. Similar results were reported by other groups, such as Ni/Au ohmic contacts to p-ZnMgO and Al/Ti ohmic contacts to Sb-doped p-type ZnO.[17,18]

## Conclusions

In this paper we fabricated low-resistivity Ni/Pt ohmic contacts on Li-doped p-type ZnO by adopting rapid thermal annealing. A lowest specific contact resistivity was $1.03 \times 10^{-4}$ Ω cm$^2$ after 550°C annealing. It is found that the current transport mechanism is tunneling-dominated for the annealed samples. We proposed that the activation of Li acceptors in ZnO film, formation of Pt–Ni solid solution near the metal surface, and a Zn-deficient p$^+$-ZnO region near the ZnO surface should be the main reasons for the formation of low-resistivity contacts. By modeling the current transport between the metal and semiconductor, we obtained a relatively low barrier height of $0.40 \pm 0.03$ eV, which confirmed that the surface states played an important role in the formation of ohmic contacts.

## Acknowledgments

This work was supported by National Basic Research Program of China under grant no. 2006CB604906, National Natural Science Foundation of China under contract no. 50532060, and the Doctoral Fund of the Ministry of Education of China under grant no. 20060335087.

*Zhejiang University assisted in meeting the publication costs of this article.*

## References

1. Y. R. Ryu, T. S. Lee, J. A. Lubguban, H. W. White, B. J. Kim, Y. S. Park, and C. J. Youn, *Appl. Phys. Lett.*, **88**, 241108 (2006).
2. Y. J. Zeng, Z. Z. Ye, W. Z. Xu, D. Y. Li, J. G. Lu, L. P. Zhu, and B. H. Zhao, *Appl. Phys. Lett.*, **88**, 062107 (2006).
3. D. C. Look, D. C. Reynolds, C. W. Litton, R. L. Jones, D. B. Eason, and G. Cantwell, *Appl. Phys. Lett.*, **81**, 1830 (2002).
4. A. Tsukazaki, A. Ohtomo, T. Onuma, M. Ohtani, T. Makino, M. Sumiya, K. Ohtani, S. F. Chichibu, S. Fuke, Y. Segawa, et al., *Nature Mater.*, **4**, 42 (2005).
5. W. Z. Xu, Z. Z. Ye, Y. J. Zeng, L. P. Zhu, B. H. Zhao, L. Jiang, J. G. Lu, H. P. He, and S. B. Zhang, *Appl. Phys. Lett.*, **88**, 173506 (2006).
6. J. H. Lim, C. K. Kang, K. K. Kim, I. K. Park, D. K. Hwang, and S. J. Park, *Adv. Mater. (Weinheim, Ger.)*, **18**, 2720 (2006); V. Vaithianathan, B. T. Lee, and S. S. Kim, *Appl. Phys. Lett.*, **86**, 062101 (2005).
7. W. Guo, A. Allenic, Y. B. Chen, X. Q. Pan, Y. Che, Z. D. Hu, and B. Liu, *Appl. Phys. Lett.*, **90**, 242108 (2007).
8. L. L. Chen, J. G. Lu, Z. Z. Ye, Y. M. Lin, B. H. Zhao, Y. M. Ye, J. S. Li, and L. P. Zhu, *Appl. Phys. Lett.*, **87**, 252106 (2005).
9. J. M. Lee, K. K. Kim, S. J. Park, and W. K. Choi, *Appl. Phys. Lett.*, **78**, 3842 (2001).
10. H. K. Kim, K. K. Kim, S. J. Park, T. Y. Seong, and I. Adesida, *J. Appl. Phys.*, **94**, 4225 (2003).
11. S. H. Kim, H. K. Kim, and T. Y. Seong, *Appl. Phys. Lett.*, **86**, 112101 (2005).
12. U. Grossner, S. Gabrielsen, T. M. Borseth, J. Grillenberger, A. Y. Kuznetsov, and B. G. Svensson, *Appl. Phys. Lett.*, **85**, 2259 (2004).
13. Y. J. Zeng, Z. Z. Ye, W. Z. Xu, L. L. Chen, D. Y. Li, L. P. Zhu, B. H. Zhao, and Y.

L. Hu, *J. Cryst. Growth*, **283**, 180 (2005).
14. L. L. Chen, H. P. He, Z. Z. Ye, Y. J. Zeng, J. G. Lu, B. H. Zhao, and L. P. Zhu, *Chem. Phys. Lett.*, **420**, 358 (2006).
15. Y. F. Lu, Z. Z. Ye, Y. J. Zeng, L. P. Zhu, and B. H. Zhao, *Electrochem. Solid-State Lett.*, **11**, H185 (2008).
16. M. G. Wardle, J. P. Goss, and P. R. Briddon, *Phys. Rev. B*, **71**, 155205 (2005).
17. H. S. Yang, Y. Li, D. P. Norton, K. Ip, S. J. Pearton, S. Jang, and F. Ren, *Appl. Phys. Lett.*, **86**, 192103 (2005).
18. L. J. Mandalapu, Z. Yang, and J. L. Liu, *Appl. Phys. Lett.*, **90**, 252103 (2007).
19. J.-J. Chen, S. Jang, T. J. Anderson, F. Ren, Y. Li, H.-S. Kim, B. P. Gila, D. P. Norton, and S. J. Pearton, *Appl. Phys. Lett.*, **88**, 122107 (2006).
20. J.-S. Jang, T.-Y. Seong, and S.-R. Jeon, *J. Appl. Phys.*, **100**, 046106 (2006).
21. J.-S. Jang, T.-Y. Seong, and S.-R. Jeon, *Appl. Phys. Lett.*, **91**, 092129 (2007).
22. S. M. Sze and K. K. Ng, *Physics of Semiconductor Devices*, 3rd ed., John Wiley & Sons, Hoboken, NJ (2007).
23. S. J. Pearton, D. P. Norton, K. Ip, Y. W. Heo, and T. Steiner, *J. Vac. Sci. Technol. B*, **22**, 932 (2004).